Journal of Biomolecular NMR

Journal of Biomolecular NMR, 5 (1995) 376–382
ESCOM

J-Bio NMR 248

Sequential backbone assignment of isotopically enriched proteins in D_2O by deuterium-decoupled HA(CA)N and HA(CACO)N

Andy C. Wang, Stephan Grzesiek, Rolf Tschudin, Patricia J. Lodi and Ad Bax

Laboratory of Chemical Physics, National Institute of Diabetes and Digestive and Kidney Diseases, National Institutes of Health, Bethesda, MD 20892-0520, U.S.A.

Received 16 September 1994
Accepted 25 October 1994

Keywords: Deuterium; Triple resonance; Isotope labeling; Sequential assignment; Ubiquitin

ESCOM

Journal of Biomolecular NMR, 5 (1995) 376–382
ESCOM

J-Bio NMR 248

Sequential backbone assignment of isotopically enriched proteins in D_2O by deuterium-decoupled HA(CA)N and HA(CACO)N

Andy C. Wang, Stephan Grzesiek, Rolf Tschudin, Patricia J. Lodi and Ad Bax

Laboratory of Chemical Physics, National Institute of Diabetes and Digestive and Kidney Diseases, National Institutes of Health, Bethesda, MD 20892-0520, U.S.A.

Received 16 September 1994
Accepted 25 October 1994

Keywords: Deuterium; Triple resonance; Isotope labeling; Sequential assignment; Ubiquitin

Summary

It is demonstrated that sequential resonance assignment of the backbone $^1H^\alpha$ and ^{15}N resonances of proteins can be obtained without recourse to the backbone amide protons, an approach which should be useful for assignment of regions with rapidly exchanging backbone amide protons and for proteins rich in proline residues. The method relies on the combined use of two 2D experiments, HA(CA)N and HA(CACO)N or their 3D analogs, which correlate $^1H^\alpha$ with the intraresidue ^{15}N and with the ^{15}N resonance of the next residue. The experiments are preferably conducted in D_2O, where very high resolution in the ^{15}N dimension can be achieved by using ^2H decoupling. The approach is demonstrated for a sample of human ubiquitin, uniformly enriched in ^{13}C and ^{15}N. Complete backbone and $^{13}C^\beta/^1H^\beta$ resonance assignments are presented.

Introduction

Backbone amide protons play a pivotal role in all homonuclear and heteronuclear protein sequential resonance assignment strategies proposed to date. They owe this role to their intraresidue J connectivity to H^α and to the fact that they frequently exhibit both intraresidue and sequential NOEs (Wüthrich, 1986), and in isotopically enriched proteins they can be conveniently correlated with many of the other backbone and side-chain atoms (Ikura et al., 1990). However, neither assignment strategy is applicable if the amide proton cannot be observed and this has been a primary reason why many protein NMR studies are restricted to a solvent pH of less than about 7, a value at which amide protons exchange sufficiently slowly to allow observation of their resonances. The present paper describes an alternative triple-resonance procedure which does not make use of backbone amide protons and which therefore can be used to study proteins at any pH.

The new procedure relies on the use of two triple-resonance experiments, HCAN and HCA(CO)N. Both schemes are of the so-called 'out-and-back' type, where magnetization originates on $^1H^\alpha$ and is transferred to ^{15}N where it evolves during an evolution period, t_1, prior to being transferred back to $^1H^\alpha$ for detection. The HCA(CO)N experiment has been described previously (Kay et al., 1990; Powers et al., 1991) and correlates $^1H^\alpha/^{13}C^\alpha$ of one residue with the backbone amide ^{15}N of the next residue, using relay of magnetization via the well-resolved $^1J_{C\alpha CO}$ and $^1J_{CON}$ couplings. The analogous HCAN experiment transfers magnetization between $^{13}C^\alpha$ and ^{15}N via $^1J_{C\alpha N}$ (intraresidue) and $^2J_{C\alpha N}$ (interresidue) and correlates $^1H^\alpha$ and $^{13}C^\alpha$ with the intraresidue and sequential ^{15}N resonances. The transfer in this latter experiment is relatively inefficient, not only because of the relatively small values of $^1J_{C\alpha N}$ (~10 Hz) and $^2J_{C\alpha N}$ (~7 Hz) (Delaglio et al., 1991) but also because $^{13}C^\alpha$ magnetization decays rapidly during the correspondingly long de- and rephasing delays, owing to its inherently short transverse relaxation time. Nevertheless, for proteins with rotational correlation times of less than ~8 ns we find that both the HCAN and the HCA(CO)N experiments, as described here, are readily applicable.

The HCAN experiment provides intraresidue (and weaker interresidue) connectivities between the $^1H^\alpha$, $^{13}C^\alpha$ and ^{15}N nuclei, whereas the HCA(CO)N correlates the $^1H^\alpha$, $^{13}C^\alpha$ of one residue with the ^{15}N of the next residue.

0925-2738/$ 6.00 + 1.00 © 1995 ESCOM Science Publishers B.V.

Use of these two experiments for sequential resonance assignment relies on the uniqueness of the ^{15}N chemical shift for making the sequential connectivity, i.e., it is critical that the ^{15}N chemical shift is measured with the highest possible precision. Backbone amide deuterons in proteins with a rotational correlation time shorter than 8 ns have T_1 relaxation times in the 2–20 ms range, owing to their ~200 kHz quadrupole coupling. In the absence of ^{2}H decoupling, scalar relaxation of the second kind therefore severely broadens the ^{15}N resonance (Pople, 1958; Abragam, 1961) and the lack of high ^{15}N resolution has previously discouraged the use of the HCA(CO)N experiment. It is therefore desirable to narrow the ^{15}N resonances by the use of broadband ^{2}H decoupling. Deuterated ^{15}N nuclei are not subject to the otherwise dominant one-bond ^{1}H-^{15}N dipolar relaxation mechanism and, as demonstrated in the present study, excellent ^{15}N resolution can be obtained when using ^{2}H decoupling.

Experimental

Two-dimensional HA(CA)N and HA(CACO)N experiments have been recorded on a sample of 4.1 mg of commercially obtained human ubiquitin, uniformly enriched in ^{13}C and ^{15}N (VLI Research, Southeastern, PA). The sample was lyophilized from D_2O, pH 9, after incubation at 35 °C for 24 h to ensure complete backbone amide exchange. It then was dissolved in 250 µl D_2O, containing deuterated acetate buffer, and the pH was adjusted to 4.7 (uncorrected for the isotope effect) by addition of a small amount of DCl, after which the sample was transferred into a Shigemi microcell NMR tube (Shigemi Inc., Allison Park, PA). The final buffer concentration was 20 mM acetic acid, 17 mM sodium acetate and 32 mM sodium chloride. Additional 3D triple-resonance experiments were carried out on a sample containing 3 mg $^{13}C/^{15}N$-ubiquitin dissolved in 250 µl 90% H_2O/10% D_2O, deuterated acetic acid buffer (36 mM acetic acid, 27 mM sodium acetate), pH 4.7.

All NMR experiments were conducted at 30 °C on a Bruker AMX-600 spectrometer, equipped with an external 150-W class A/B power amplifier for ^{13}C and a Bruker digital lock and triple-resonance probehead with a self-shielded z-gradient. Pulsed field gradients were generated with an in-house developed gradient pulse-shaping unit and amplifier. All gradient pulses were sine-bell shaped, with a strength of 25 G/cm at the center of the sine bell. ^{2}H decoupling was applied using the regular ^{2}H lock probehead circuitry and the rf power was produced using a home-built rf channel, shown schematically in Fig. 1. The ^{2}H decoupling rf originated from a PTS 300 synthesizer that was switched from the local mode, when ^{2}H decoupling is desired, to remote control when no output is needed, thereby switching its output frequency to 0 Hz and minimal power. The 10 MHz reference for this synthesizer was derived from the console. After additional gating and amplification, the ^{2}H decoupling power was sent to the probe through a 3 dB coupler (Merrimac PDH-20-250). The regular lock signal was sent through the other port of the coupler via an active dual gate

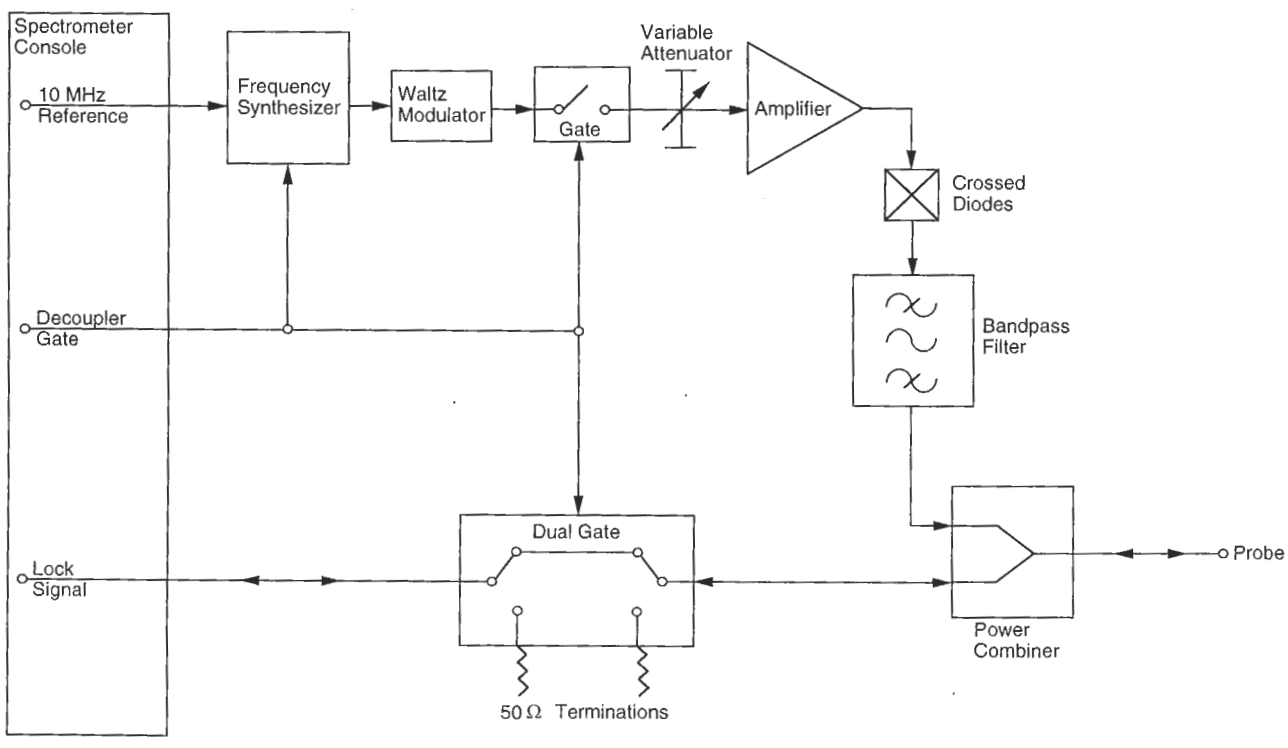

Fig. 1. Simplified block diagram of the deuterium decoupling hardware used in this work.

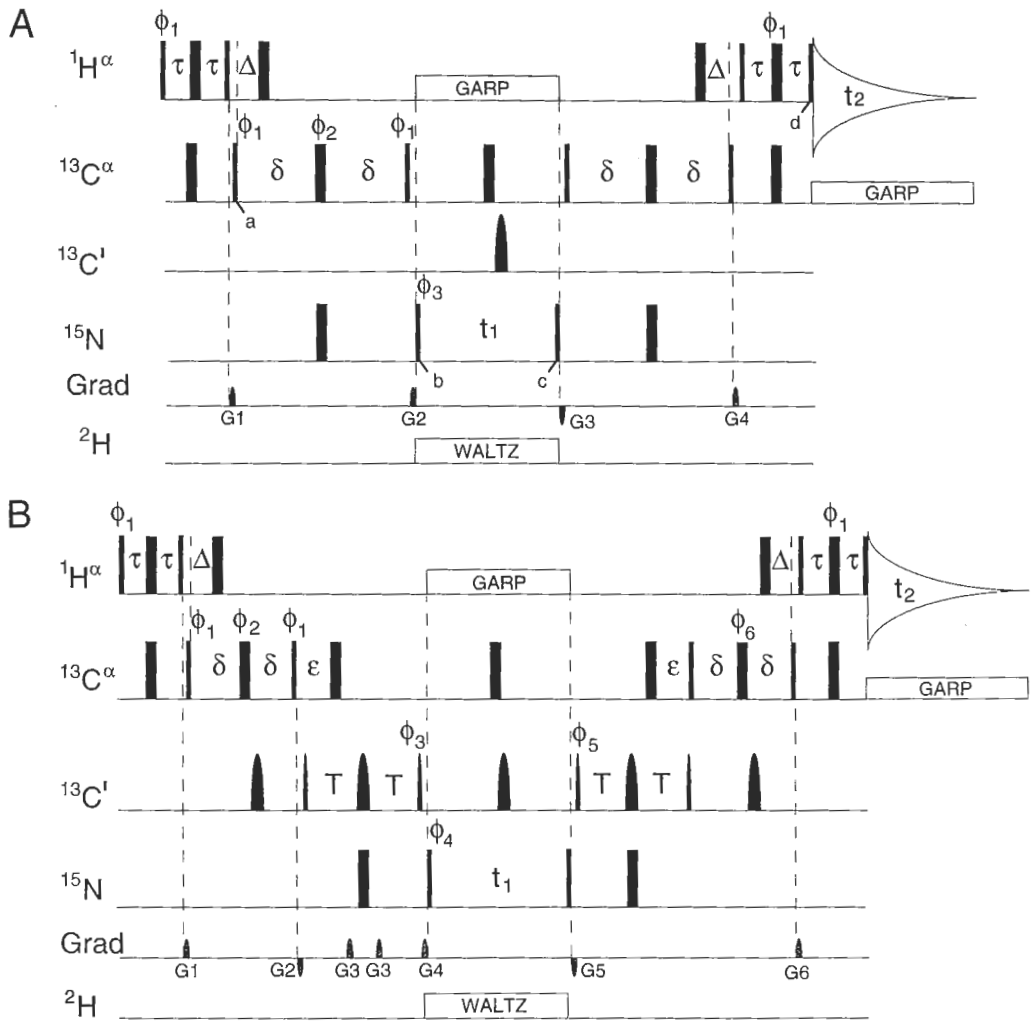

Fig. 2. Pulse sequences of the (A) HA(CA)N and (B) HA(CACO)N experiments. Narrow and wide pulses correspond to 90° and 180° flip angles, respectively. Pulses for which the phase is not indicated are applied along the x-axis. The ^1H carrier is placed at the H_2O frequency. ^1H broadband decoupling is accomplished with a synchronous GARP sequence (Shaka et al., 1985) using a 1 kHz rf field. ^2H decoupling (2 W) utilized a WALTZ-modulated (Shaka et al., 1983) composite pulse sequence and a 1.7 kHz rf field, centered in the amide region. ^{13}C decoupling during data acquisition was performed with a GARP sequence using a 5 kHz rf field. The carriers for the $^{13}C^\alpha$ and $^{13}C'$ pulses are positioned at 56 and 177 ppm, respectively. The power levels of the 90° and 180° $^{13}C^\alpha$ pulses, 4.7 and 10.6 kHz, are adjusted such that they do not excite the $^{13}C'$ nuclei. Carbonyl pulses have a shaped amplitude profile, corresponding to the center lobe of a sinx/x function, and a duration of 157 and 84 μs for the 180° and 90° pulses, respectively. Phase cycling is as follows: (A) $\phi_1 = y$; $\phi_2 = x,y$; $\phi_3 = x,x,-x,-x$; Acq. = x,−x,−x,x; and (B) $\phi_1 = y$; $\phi_2 = 80°,170°$; $\phi_3 = 48°$; $\phi_4 = x,x,-x,-x$; $\phi_5 = 132°$; $\phi_6 = 80°$; Acq. = x,−x,−x,x. Quadrature detection in the t_1 domain is obtained by changing the phases ϕ_3 (A) and ϕ_4 (B) in the usual States-TPPI manner (Marion et al., 1989). Delay durations for (A) are $\tau = 1.5$ ms, $\Delta = 1.55$ ms and $\delta = 14.28$ ms, and those for (B) are $\tau = 1.5$ ms, $\Delta = 1.55$ ms, $\delta = 3.2$ ms, $\varepsilon = 4.5$ ms and $T = 13.1$ ms. Pulsed field gradient durations for (A) are G1 = 1.5 ms, G2 = 0.5 ms (negative polarity), G3 = 0.75 ms (negative polarity) and G4 = 1.25 ms, and those for (B) are G1 = 1.5 ms, G2 = 0.5 ms (negative polarity), G3 = 0.1 ms, G4 = 0.25 ms, G5 = 0.75 ms (negative polarity) and G6 = 1.25 ms.

which terminates both the combiner and the lock channel in 50 Ω. This dual gate protects the lock circuitry during the ^2H decoupling period. In addition, the ^2H lock receiver is blanked during ^2H decoupling. A home-built WALTZ (Shaka et al., 1983) modulator circuit was used to ensure uniform ^2H decoupling over the amide region. In practice, however, we found the use of this WALTZ modulation scheme to be only of marginal benefit because the short T_1 of the ubiquitin amide deuterons (6–9 ms) acts as 'noise modulation'. Even when using a continuous-wave ^2H decoupling field, this T_1 modulation therefore results in adequate ^2H decoupling over a 4 ppm ^2H bandwidth when using a ^2H rf field strength of 1.7 kHz (2 W).

The 2D HA(CA)N and HA(CACO)N spectra were collected as 512* (t_1) × 256* (t_2) data sets (where n* refers to n complex data points), with acquisition times of 389 ms (t_1) and 85 ms (t_2). With a relaxation delay of 1.2 s, the total measuring time was 2 h for each experiment. The ^2H lock receiver and lock transmitter are active only during the 1.2 s relaxation delay. Prior to Fourier transformation, the data were apodized with a squared sine-

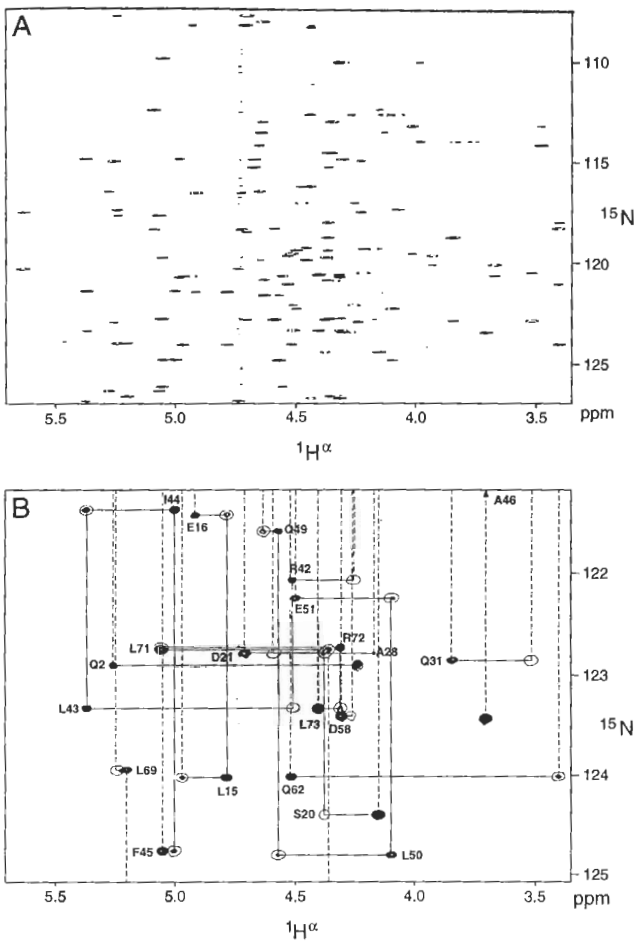

Fig. 3. Superimposed regions of the 2D HA(CA)N and HA(CACO)N spectra of human ubiquitin. (A) View of all resonances; (B) expansion of a selected region. The entire HA(CACO)N spectrum was multiplied by −1 prior to superposition; positive correlations are shown with multiple contours and negative peaks are drawn with a single contour. Therefore, HA(CA)N correlations are mostly positive and HA(CACO)N correlations are mostly negative, with peaks aliased in the ^{15}N dimension having the opposite sign (e.g. Ser^{20}). Intraresidue ^{1}H$^{\alpha}$-^{15}N correlations are identified by residue number. Weaker interresidue ^{1}H$^{\alpha}$-^{15}N correlations are also observed in the HA(CA)N spectrum and their position coincides with that of the more intense HA(CACO)N cross peaks. Horizontal lines connect [^{1}H$^{\alpha}$(i)/^{15}N(i)] and [^{1}H$^{\alpha}$(i−1)/^{15}N(i)] correlations and vertical lines connect [^{1}H$^{\alpha}$(i−1)/^{15}N(i)] and [^{1}H$^{\alpha}$(i−1)/^{15}N(i−1)] correlations; together they trace out the sequential ^{1}H$^{\alpha}$/^{15}N assignment of the protein backbone.

bell function shifted by 59° in both dimensions, and then zero-filled to 2048* along t_1 and 1024* along t_2. Data were processed using the package nmrPipe (Delaglio, F., unpublished results) and peak positions and intensities for non-overlapping resonances were determined interactively using the program PIPP (Garrett et al., 1991).

Results and Discussion

Figure 2 shows the pulse sequences of the 2D HA-(CA)N and HA(CACO)N experiments used in the present work. For proteins as small as ubiquitin (8.5 kDa) there is little degeneracy in the ^{1}H$^{\alpha}$ chemical shifts and the 2D versions provide sufficient resonance dispersion. For larger proteins, or for proteins with less resolved ^{1}H$^{\alpha}$ shifts, the experiments can be recorded in a 3D manner by converting the ^{13}C$^{\alpha}$ dephasing period into a constant-time type evolution period.

The magnetization transfer pathway pertinent to the HA(CA)N experiment will be briefly outlined below. For simplicity, only terms that contribute to the final spectrum are retained and the effects of relaxation are ignored. The first 90° (^{1}H) − τ − 180° (^{1}H,^{13}C) − τ − 90° (^{1}H, ^{13}C) comprises an INEPT transfer (Morris and Freeman, 1979) from ^{1}H$^{\alpha}$ to ^{13}C$^{\alpha}$, and the magnetization at time point a is described by $2H_z^{\alpha}C_x^{\alpha}$. During the subsequent delay of duration 2δ, $^{1}J_{H\alpha C\alpha}$ rephasing is active for a period 2Δ and ^{13}C$^{\alpha}$-^{15}N dephasing occurs due to $^{1}J_{C\alpha N}$ and $^{2}J_{C\alpha N}$. During this period, ^{13}C$^{\alpha}$ also dephases with respect to ^{13}C$^{\beta}$, but by setting 2δ to $1/{}^{1}J_{C\alpha C\beta}$ the net effect is merely an inversion of the ^{13}C$^{\alpha}$ magnetization, which will be ignored in the following discussion. At the end of period 2δ, ^{13}C$^{\alpha}$ magnetization is transferred by INEPT partly to the intraresidue ^{15}N (N^{i}) and also to the sequential ^{15}N (N^{i+1}). Magnetization at time point b is then described by the sum of two terms, i.e., $2\sin(2\pi\delta\,{}^{1}J_{C\alpha N^{i}})\cos(2\pi\delta\,{}^{2}J_{C\alpha N^{i+1}})\,C_z^{\alpha}N_y^{i} + 2\cos(2\pi\delta\,{}^{1}J_{C\alpha N^{i}})\sin(2\pi\delta\,{}^{2}J_{C\alpha N^{i+1}})\,C_z^{\alpha}N_y^{i+1}$. For reasons of brevity only the fate of the first term will be discussed below, although, of course, the second term undergoes the same type of transfer. At the end of the t_1 period, a fraction $\cos(\Omega_{N^{i}}t_1)$ of the N^{i} magnetization is transferred back to ^{13}C$^{\alpha}$ (time c) where, after a refocusing period 2δ, it is transferred by reverse INEPT back to ^{1}H$^{\alpha}$ for detection. The observed ^{1}H$^{\alpha}$ signal then originates from the following term:

$$S(t_1,t_2) = \sin^2(2\pi\delta\,{}^{1}J_{C\alpha N^{i}})\cos^2(2\pi\delta\,{}^{2}J_{C\alpha N^{i+1}}) \times \cos(\Omega_{N^{i}}t_1)\exp(i\,\Omega_{H\alpha}t_2) \quad (1)$$

which after 2D Fourier transformation yields the intraresidue ^{1}H$^{\alpha}$-^{15}N correlation. The last 90° ^{1}H pulse, applied at time point d, does not affect the ^{1}H$^{\alpha}$ magnetization, which is aligned parallel to the x-axis at this time (Madsen et al., 1993), but it returns any transverse HDO magnetization back to the z-axis, thereby significantly reducing the t_1 noise originating from this intense signal.

The HA(CACO)N experiment (Fig. 2B) used in the present work is a 2D analog of a previously described scheme (Kay et al., 1990; Powers et al., 1991; Palmer et al., 1992), slightly modified by the added ^{2}H decoupling, incorporation of pulsed field gradients, and a final water-flip-back pulse immediately prior to detection. Also, magnetization transfer from ^{13}C' to ^{15}N is accomplished with an INEPT instead of an HMQC scheme. One other detail concerns the compensation of the effects of the Bloch–Siegert shift (Freeman, 1988) induced by the application of a ^{13}C' 180° pulse during ^{13}C$^{\alpha}$ evolution, and vice

TABLE I
BACKBONE AND $^{13}C^{\beta}/^{1}H^{\beta}$ RESONANCE ASSIGNMENTS OF HUMAN UBIQUITIN[a]

Residue	^{15}N	$^{13}C{=}O$	$^{13}C^{\alpha}$	$^{13}C^{\beta}$	$^{1}H^{N}$	$^{1}H^{\alpha}$	$^{1}H^{\beta}$
M1	–	170.54	54.54	33.29	[b]	4.22	2.13[c], 2.11[c]
Q2	123.22	175.92	55.19	30.76	8.90	5.26	1.86, 1.66
I3	115.34	172.45	59.65	42.21	8.32	4.19	1.79
F4	118.11	175.32	55.29	41.43	8.61	5.64	3.05, 2.88
V5	121.00	174.87	60.69	34.25	9.30	4.74	1.92
K6	127.52	177.14	54.61	34.86	8.82	5.36	1.68, 1.35
T7	115.40	176.91	60.64	70.63	8.73	4.95	4.83
L8	121.33	178.80	57.69	42.04	9.10	4.31	1.93, 1.78
T9	105.59	175.52	61.51	69.18	7.63	4.43	4.59
G10	108.89	174.07	45.46	–	7.81	4.35	3.61[d]
K11	121.60[c]	175.94	56.43	33.37	7.28	4.35	1.82, 1.72
T12	120.44	174.32	62.51	69.93	8.65	5.03	3.95
I13	127.11	175.22	60.10	40.92	9.45	4.53	1.88
T14	121.52	173.79	62.16	69.70	8.71	4.97	4.04
L15	124.80	174.67	52.93	47.05	8.71	4.76	1.36, 1.22
E16	122.16	175.86	54.96	29.61	8.14	4.90	1.94, 1.84
V17	117.21	174.16	58.53	36.40	8.90	4.72	2.33
E18	118.99	176.14[e]	52.80	30.47	8.64	5.08	2.18[c,f], 1.62
P19	133.94[e]	175.31	65.42	31.96	–	4.14[c]	2.45, 2.01[c]
S20	103.40[c]	174.66	57.48	63.51	7.04	4.37	4.17, 3.80
D21	123.48	176.36	55.83	40.87	8.03	4.70	2.95, 2.55[c]
T22	108.80	176.75	59.83	71.32	7.90	4.91	4.82
I23	121.19	179.04	62.40	34.51	8.56	3.65	2.54
E24	120.83	178.64	60.48	28.43	9.72	3.92	2.05, 2.05[c]
N25	120.57	178.38	56.18	38.58	7.92	4.53	3.22, 2.88
V26	121.71	177.95	67.75	30.87	8.07	3.40	2.36
K27	118.86	180.55	59.36	33.78	8.56	4.57	2.04, 1.45[c,f]
A28	123.44	180.30	55.46	17.78	8.06	4.16	1.64
K29	119.94	180.32	59.86	33.36	7.85	4.20	2.14, 1.94[c,f]
I30	121.08	178.31	66.20	36.88	8.28	3.51	2.37
Q31	123.49	178.89	60.12	27.82	8.58	3.83	2.50, 1.99[c]
D32	119.36	177.25	57.39	40.78	8.01	4.36	2.88[c], 2.80
K33	115.13	177.87	58.16	34.11	7.43	4.34	2.01[c], 1.86
E34	113.87	177.84	55.36	32.95	8.74	4.61	2.28, 1.71
G35	108.65	173.96	46.19	–	8.53	4.14	3.93[d]
I36	119.88	173.57[e]	57.85	40.62	6.15	4.44	1.43
P37	141.40[e]	176.92[e]	61.76[c]	[b]	–	4.60[c]	[b]
P38	135.09[e]	178.32	66.25	32.90	–	4.12	2.23, 2.06
D39	113.38	177.09	55.82	39.69	8.55	4.42	2.80, 2.70
Q40	116.78	175.38	55.69	30.18	7.82	4.47	2.47[c,f], 1.84
Q41	117.72	176.30	56.68	31.65	7.48	4.24	1.93, 1.93
R42	122.68	174.05	55.19	31.81	8.53	4.50	1.72, 1.61[c]
L43	124.04	175.29	53.10	45.80	8.82	5.35	1.58, 1.15[c]
I44	121.92	176.06	59.05	41.35	9.03	4.99	1.70
F45	125.39	174.47	57.02	43.85	8.83	5.03	3.04, 2.82
A46	132.20	177.29	52.67	16.61	8.81	3.69	0.91
G47	102.34	173.81	45.46	–	8.13	4.09	3.45[d]
K48	121.57	174.70	54.72	34.60	7.98	4.62	1.90, 1.90[c,f]
Q49	122.41	175.67	55.86	29.18	8.60	4.56	1.99, 1.99[c,f]
L50	125.52	176.66	54.36	41.53	8.53	4.08	1.50, 1.03
E51	122.94	175.87	56.07	31.72	8.40	4.49	2.24[c], 2.01
D52	120.03	177.33	56.98	40.91	8.16	4.37	2.68[f], 2.56[f]
G53	106.66	174.87	45.33	–	9.36	4.14	3.98[d]
R54	119.05	175.35	54.44	32.73	7.46[c]	4.71[c]	2.24[c], 2.09[c]
T55	108.40	176.56	59.82	72.43	8.73	5.24	4.56
L56	117.92	180.81	58.82	40.39	8.14	4.06	2.12, 1.23
S57	113.33	178.31	61.19	62.64	8.47	4.26	3.85, 3.76
D58	124.19	177.40	57.40	40.18	7.93	4.30	3.02, 2.31
Y59	115.51	174.70	58.35	40.09	7.25	4.66	3.47, 2.54
N60	115.90	174.34	54.24	37.50	8.15	4.36	3.32, 2.80
I61	118.60	174.61	62.52	36.71	7.25	3.40	1.41
Q62	124.74	175.97	53.73	31.72	7.61	4.50	2.27[c], 1.91

TABLE 1
(continued)

Residue	^{15}N	$^{13}C{=}O$	$^{13}C^{\alpha}$	$^{13}C^{\beta}$	$^{1}H^{N}$	$^{1}H^{\alpha}$	$^{1}H^{\beta}$
K63	120.30	175.81	58.00	32.70	8.49	3.99	2.05, 1.91
E64	113.95	175.25	58.14	25.97	9.28	3.43	2.58, 2.45
S65	114.73	172.16	61.08	65.04	7.67	4.64	3.90, 3.65
T66	117.11	173.95	62.49	70.24	8.73	5.28	4.08
L67	127.11	175.77	53.93	44.34	9.41	5.07	1.63, 1.63[f]
H68	118.38	173.15	55.25	30.88	9.23	5.20	3.20[e], 3.00
L69	124.46	175.27	54.04	44.41	8.34	5.19	1.62, 1.11[e]
V70	126.94	174.00	60.83	34.94	9.20	4.36	2.03
L71	123.13	177.83	54.08	42.93	8.12	5.05	1.68[f], 1.55
R72	123.49	175.35	55.79	31.37	8.58	4.28	1.76, 1.54
L73	124.22	177.45	54.97	42.60	8.32	4.40	1.63[e], 1.58[f]
R74	121.45	176.87	56.71	30.71	8.39	4.29	1.86, 1.81
G75	110.78	173.68	45.35	–	8.45	3.98	3.98[d]
G76	114.68	179.13[e]	46.10	–	7.92	3.82	3.75[d]

[a] The sample was 1.4 mM in H_2O, acetic acid buffer (36 mM acetic acid, 27 mM sodium acetate), pH 4.7, 30 °C. ^{1}H chemical shifts are indirectly referenced to TSP by using the water reference as an internal standard at 4.72 ppm. ^{13}C chemical shifts are also relative to TSP, where the 0 ppm value has been obtained by multiplication of the ^{1}H TSP frequency by 0.25144954 (Bax and Subramanian, 1986). ^{15}N chemical shifts are relative to liquid ammonia at 25 °C, where the 0 ppm value has been obtained by multiplication of the ^{1}H TSP frequency by 0.10132914 (Live et al., 1984). Except for prolines, chemical shifts correspond to protonated ^{15}N.

[b] Not assigned.

[c] Chemical shift differs from that given in DiStefano and Wand (1987).

[d] Chemical shift of the second glycine $^{1}H^{\alpha}$.

[e] Shifts obtained from the HA(CA)N, HA(CACO)N or HCACO experiments, recorded in D_2O.

[f] Chemical shift differs from that given in Weber et al. (1987).

versa (McCoy and Mueller, 1992; Vuister and Bax, 1992), which occurs at four different points in the pulse sequence (the midpoints of the 2δ and 2T durations). During application of a $^{13}C'$ 180° pulse, the $^{13}C^{\alpha}$ spin changes its precession frequency, resulting in an additional rotation about the z-axis which, to a first approximation, is proportional to the strength of the 180° $^{13}C'$ pulse, i.e., inversely proportional to its width. This additional rotation by an angle θ can be compensated for by reducing the phase of the 180° $^{13}C^{\alpha}$ pulse by θ/2 (as done for the $^{13}C^{\alpha}$ $180^{\circ}_{\phi 2/\phi 6}$ pulses), by increasing the phase of the 90° pulse at the end of this period by θ (as done for $^{13}C'$ $90^{\circ}_{\phi 3}$) or by decreasing the phase of the 90° pulse at the beginning of the de-/rephasing period ($90^{\circ}_{\phi 5}$).

The two-dimensional ^{2}H-decoupled HA(CA)N and HA(CACO)N spectra of ubiquitin are shown superimposed in Fig. 3. The long ^{15}N T_2 relaxation times (~300 ms as measured from ^{2}H-decoupled CPMG T_2 measurements; data not shown) allow the spectra to be recorded with very high ^{15}N resolution, removing any spectral degeneracy in this dimension. Due to the choice of the duration of Δ (~ 1/4 $^{1}J_{C\alpha H\alpha}$), glycine $^{13}C^{\alpha}$ magnetization is not refocused with respect to its attached protons at the end of the first 2δ period in either the HA(CA)N or HA(CACO)N schemes and glycine signals are therefore vanishingly weak in Fig. 3 (Burum and Ernst, 1980). The resulting glycine 'gaps' in the HA(CA)N and HA(CACO)N sequential assignment pathway can actually facilitate the assignment process: knowledge of the primary sequence allows Gly^{i} to Gly^{i+n} stretches to be easily identified, as long as no two stretches are of identical length. Resonance assignments are summarized in Table 1.

Ubiquitin is a stable and well-characterized protein and it is presently the only protein commercially available in a uniformly $^{13}C/^{15}N$-enriched form. It is commonly used in a number of laboratories to optimize the performance of multidimensional multinuclear experiments. Therefore, also listed in Table 1 are the $^{1}H^{\alpha}$, $^{1}H^{\beta}$, $^{13}C^{\alpha}$, $^{13}C^{\beta}$ and $^{13}C'$ chemical shifts, obtained from two-scan versions of the HBHA(CO)NH (Grzesiek and Bax, 1993), HBHANH (Wang et al., 1994), CBCA(CO)NH (Grzesiek and Bax, 1992a), CBCANH (Grzesiek and Bax, 1992b), HCACO (Grzesiek and Bax, 1993) and HNCO (Grzesiek and Bax, 1992c) experiments which were optimized on a 1.4 mM ubiquitin sample dissolved in H_2O. In the course of this work, we noticed that several of the ^{15}N, $^{1}H^{N}$ and $^{1}H^{\alpha}$ chemical shifts are quite sensitive to sample concentration, pH and ionic strength. However, except for the ^{15}N shifts of Lys^{11} and Ser^{20} and several of the $^{1}H^{\beta}$ resonances, assignments are in general agreement with those reported previously (DiStefano and Wand, 1987; Weber et al., 1987; Schneider et al., 1992).

For proteins dissolved in D_2O, the ^{15}N line narrowing resulting from $^{2}H^{N}$ decoupling allows the collection of highly resolved ^{15}N spectra, thereby facilitating the assignment process. For small proteins such as ubiquitin, virtually complete sequential assignment of the $^{1}H^{\alpha}$ and ^{15}N spectra can be made on the basis of two triple-resonance 2D spectra, HA(CA)N and HA(CACO)N, requiring a combined measuring time of only 4 h. For proteins at

high pH or rich in proline residues, this type of D_2O experiments provides a valuable complement to the large range of amide proton-based triple-resonance J connectivity experiments.

Acknowledgements

We thank Dennis Torchia, Marius Clore, Angela Gronenborn, Frank Delaglio, John Marquardt, James Ernst and Geerten Vuister for stimulating discussions, and Dan Garrett and Frank Delaglio for developing the software used to analyze and process the NMR data. This work was supported by the AIDS Targeted Anti-Viral Program of the Office of the Director of the National Institutes of Health. A.C.W. is supported by an American Cancer Society postdoctoral fellowship (PF-4030). P.J.L. is supported by a Cancer Research Institute/Elisa Heather Halpern postdoctoral fellowship.

References

Abragam, A. (1961) *Principles of Nuclear Magnetism*, Oxford University Press, Oxford, pp. 309, 501.

Bax, A. and Subramanian, S. (1986) *J. Magn. Reson.*, **67**, 565–569.

Burum, D.P. and Ernst, R.R. (1980) *J. Magn. Reson.*, **39**, 163–168.

Delaglio, F., Torchia, D.A. and Bax, A. (1991) *J. Biomol. NMR*, **1**, 439–446.

DiStefano, D.L. and Wand, A.J. (1987) *Biochemistry*, **26**, 7272–7281.

Freeman, R. (1988) *A Handbook of Nuclear Magnetic Resonance*, Longman, New York, NY, pp. 14–16.

Garrett, D.S., Powers, R., Gronenborn, A.M. and Clore, G.M. (1991) *J. Magn. Reson.*, **95**, 214–220.

Grzesiek, S. and Bax, A. (1992a) *J. Am. Chem. Soc.*, **114**, 6291–6293.

Grzesiek, S. and Bax, A. (1992b) *J. Magn. Reson.*, **99**, 201–207.

Grzesiek, S. and Bax, A. (1992c) *J. Magn. Reson.*, **96**, 432–440.

Grzesiek, S. and Bax, A. (1993) *J. Magn. Reson. Ser. B*, **102**, 103–106.

Ikura, M., Kay, L.E. and Bax, A. (1990) *Biochemistry*, **29**, 4659–4667.

Kay, L.E., Ikura, M., Tschudin, R. and Bax, A. (1990) *J. Magn. Reson.*, **89**, 496–514.

Live, D.H., Davis, D.G., Agosta, W.C. and Cowburn, D. (1984) *J. Am. Chem. Soc.*, **106**, 1939–1941.

Madsen, J.C., Sørensen, O.W., Sørensen, P. and Poulsen, F.M. (1993) *J. Biomol. NMR*, **3**, 239–244.

Marion, D., Ikura, M., Tschudin, R. and Bax, A. (1989) *J. Magn. Reson.*, **85**, 393–399.

McCoy, M.A. and Mueller, L. (1992) *J. Magn. Reson.*, **99**, 18–36.

Morris, G.A. and Freeman, R. (1979) *J. Am. Chem. Soc.*, **101**, 760–762.

Palmer, A.G., Fairbrother, W.J., Cavanagh, J., Wright, P.E. and Rance, M. (1992) *J. Biomol. NMR*, **2**, 103–108.

Pople, J.A. (1958) *Mol. Phys.*, **1**, 168–174.

Powers, R., Gronenborn, A.M., Clore, G.M. and Bax, A. (1991) *J. Magn. Reson.*, **94**, 209–213.

Schneider, D.M., Dellwo, M.J. and Wand, A.J. (1992) *Biochemistry*, **31**, 3645–3652.

Shaka, A.J., Barker, P.B. and Freeman, R. (1983) *J. Magn. Reson.*, **53**, 313–340.

Shaka, A.J., Barker, P.B. and Freeman, R. (1985) *J. Magn. Reson.*, **64**, 547–552.

Vuister, G.W. and Bax, A. (1992) *J. Magn. Reson.*, **98**, 428–435.

Wang, A.C., Lodi, P.J., Qin, J., Vuister, G.W., Gronenborn, A.M. and Clore, G.M. (1994) *J. Magn. Reson. Ser. B*, **105**, 196–198.

Weber, P.L., Brown, S.C. and Mueller, L. (1987) *Biochemistry*, **26**, 7282–7290.

Wüthrich, K. (1986) *NMR of Proteins and Nucleic Acids*, Wiley, New York, NY.